

Theoretical spin-orbit coupling constants for 3d ions in crystals

E. Francisco and L. Pueyo

Departamento de Química Física y Analítica, Universidad de Oviedo, 33007 Oviedo, Spain

(Received 10 August 1987)

Theoretical spin-orbit constants for the V^{2+} , Cr^{z+} ($z = 1-3$), and Mn^{2+} ions in $KMgF_3$ have been calculated by means of the theory of Blume and Watson [Proc. R. Soc. London, Ser. A **270**, 127 (1962); **271**, 565 (1963)] and the approximate cluster Hamiltonian of Misetich and Buch [J. Chem. Phys. **41**, 2524 (1964)]. The modified one-center spin-orbit parameters appearing in the latter Hamiltonian have been obtained by means of Hartree-Fock-Roothaan calculations on the octahedral MF_6 clusters (M is the 3d ion) including the cluster-lattice interaction. The 3d-orbital deformation, deduced from the cluster calculations, appears as a key factor in determining the spin-orbit constants and their reduction with respect to the free-ion values. Covalency effects are less important in this highly ionic compound. Ligand contributions to the spin-orbit constants are smaller than 10%. The variation of these constants with the metal-ligand distance R has also been determined from calculations at different values of R . According to the results of this and previous work, the spin-orbit constants behave as local observables, fairly independent of the effects of the rest of the lattice on the cluster wave function. The theoretical coupling constants agree rather well with available experimental values.

INTRODUCTION

The analysis of the optical spectrum of the transition-metal ions in crystals generally requires consideration of spin-orbit coupling. In 3d ions this interaction represents a fraction (between 0.1 and 0.01) of the 3d-3d electron-repulsion energy but its effects are quite substantial. As is well known,¹ spin-orbit coupling may split the electronic states of the transition-metal ion, giving structure to the spectral bands, and can mix electronic states of different spin multiplicity giving rise to a partial relaxation of the $\Delta S=0$ selection rule. Thus electronic transitions which are forbidden in the absence of spin-orbit coupling may borrow intensity from some nearby spin-allowed transition through the spin-orbit mixing. This interaction is also important in the interpretation of the electron resonance spectra of these systems^{1,2} since it contributes to the g factors, zero-field splitting, and line shapes.

Unfortunately, accurate spin-orbit constants are only rarely available as experimental observables in a crystal or molecular environment. For instance, the determination of these constants from the observed fine structure of the optical spectra is generally complicated by the presence of other perturbations of analogous size, such as low-symmetry fields¹ or Jahn-Teller distortions.³

The information available on crystal spin-orbit constants reveals that these quantities are generally smaller than their free-ion counterparts. This reduction was attributed by Owen⁴ to the metal-ligand orbital mixing associated to the bond formation, and, in particular, to the covalency of these bonds. On the other hand, Marshall and Stuart⁵ argued that the covalency should increase the spin-orbit constant. According to them,⁵ the observed reduction may be explained by assuming an expansion of the 3d orbitals in passing from the free ion to the crystal, in similar fashion to the reduction of electron-repulsion parameters.⁶

Radial expansion of the 3d orbitals has been invoked by Cole and Garrett⁷ to provide a correlation between the effective spin-orbit constant and the electron-repulsion parameters in both free ions and crystals. This correlation supplies a very useful device to determine spin-orbit constants from observed values of electron-repulsion parameters but, as these authors remark,⁷ it should not be interpreted as a theoretical model.

The nonempirical calculation of the spin-orbit constants in crystals has received little attention in comparison with the theoretical significance of these parameters. As a matter of fact, there have been very few examples of this type of calculation.

In an important paper, Misetich and Buch⁸ derived an approximate spin-orbit Hamiltonian adequate for transition-metal clusters from the Bethe-Salpeter Hamiltonian. The crystal spin-orbit constants derivable from the Hamiltonian of Misetich and Buch⁸ are linear combination of modified free-ion constants. Misetich and Watson⁹ carefully analyzed the molecular orbital matrix elements of this Hamiltonian, for the $Ni^{2+}:KMgF_3$ system, and showed that the multicenter integrals appearing in them are negligible. Pueyo and Richardson¹⁰ used the Misetich and Buch Hamiltonian⁸ in combination with empirical values of the free-ion constant for their study of the optical spectrum of the $(CrF_6)^{3-}$ ion in CrF_3 and K_2NaCrF_6 . Setyono and Scherz¹¹ adopted also this Hamiltonian⁸ in their recent complete neglect of differential overlap (CNDO) calculation of the spin-orbit constants for the Cu^{2+} ion in ZnS and CdS .

In this paper we report the results of our investigation of the crystal spin-orbit constants for 3d systems in the context of the Misetich and Buch approximation.⁸ It is clear that within this model the main theoretical problem is to determine the modifications of the free-ion constants. Since such modifications are due to the electronic relocation accompanying the formation of the crystal binding, we have obtained them by means of cluster cal-

culations based on Hartree-Fock-Roothaan theory. In this way, an analysis of the crystal spin-orbit constants in relation with theoretical mechanisms such as the 3d-orbital deformation, metal-ligand covalency, and other characteristics of the electronic distribution around the metal ion in the crystal may be carried out.

The one-center spin-orbit parameters resulting from the Hamiltonian of Misetich and Buch⁸ may be accurately calculated by means of the rigorous atomic theory of the spin-orbit coupling developed by Blume and Watson^{12,13} or, as we have recently shown,¹⁴ by using effective core potentials and reduced basis sets. To take care of the modifications required by Misetich and Buch,⁸ i.e., to incorporate 3d-orbital deformation effects and metal-ligand covalency, we have derived effective 3d orbitals from the molecular orbitals (MO's) determined by self-consistent-field (SCF) calculations on octahedral ML_6 clusters, M being the 3d ion and L its six nearest neighbors. These SCF calculations have been performed on the $(CrF_6)^{n-}$ ($n=3-5$), $(MnF_6)^{4-}$, and $(VF_6)^{4-}$ systems in $KMgF_3$ by following the open-shell Hartree-Fock-Roothaan methodology of Richardson *et al.*,¹⁵ with inclusion of an accurate representation of the crystal lattice.

Furthermore, the variation of the cluster spin-orbit constant with the metal-ligand distance has been obtained from these calculations. Knowledge of this variation would be an interesting piece of information in describing the modifications of the theoretical electronic spectrum due to changes in the environment of the cluster, including those produced by the application of external pressure.

Our results show that the 3d-orbital deformation is a key component of the crystal spin-orbit constant. The covalency contribution is rather small in the fluorides analyzed here but it could be much more important in oxides or chlorides. The ligand contribution to the total constant is also small. The constants computed here follow well the relations with the atomic expectation values $\langle r^{-3} \rangle$ considered by Marshall and Stuart⁵ and by Cole and Garrett.⁷ The variation of the spin-orbit constants with the metal-ligand distance is only moderate and reveals that the covalency effects are short ranged. The correlation discussed by Cole and Garrett⁷ between the spin-orbit constants and the theoretical electron-repulsion parameters is satisfied by our theoretical results for isoelectronic, isovalent, and isometallic sequences of cations. These results agree rather well with available experimental data.

The method of calculation described here permits a straightforward and reasonably accurate determination of the effects on the spin-orbit constants of different theoretical refinements in the cluster calculation. Ligand-ligand and cluster-lattice interactions, as well as improvements in the basis set, are examples of these effects. This makes the method particularly appropriate for theoretical calculations of the optical spectra of these systems. In these calculations it is not unusual to consider progressive levels of accuracy in the cluster wave function. The model presented in this work allows for an immediate transfer of this improved accuracy into the crys-

tal spin-orbit constant. This situation contrasts with those approaches in which empirical spin-orbit constants are included in otherwise very accurate spectral calculations.

THEORY

We will describe the spin-orbit interaction in the ML_6 cluster by means of the Hamiltonian of Misetich and Buch.⁸

$$H_{so} = \sum_i \xi^M(r_i) l_i \cdot s_i + \sum_{i,k} \xi^L(r_{ki}) l_{ki} \cdot s_i, \quad (1)$$

where the indices i and k run over the n electrons of the open-shell 3dⁿ system and the six ligands of the ML_6 cluster, respectively. l_i and l_{ki} are orbital angular momentum operators referred to the metal ion and to the k th ligand, and s_i is the electron spin angular momentum operator. $\xi^M(r_i)$ and $\xi^L(r_{ki})$ are modified spin-orbit functions of the metal and ligand free ions. In the simplest form they can be expressed in terms of a one-electron operator:¹⁶

$$\xi(r) = \frac{1}{2} \alpha^2 \frac{1}{r} \frac{\partial V(r)}{\partial r}, \quad (2)$$

α being the fine structure constant and $V(r)$ the central field seen by the valence electron. An alternative and accurate way of representing these functions can be formulated in terms of effective core potentials and reduced basis sets.¹⁴ The word "modified" in the context of the theory of Misetich and Buch⁸ implies the consideration of the cluster electron density instead of the free-ion density. We describe below how to incorporate such modification.

If we write H_{so} in the form

$$H_{so} = \sum_i t_i \cdot s_i, \quad (3)$$

where

$$t_i = \xi^M(r_i) l_i + \sum_k \xi^L(r_{ki}) l_{ki}, \quad (4)$$

its matrix elements in the strong-field $|\alpha S \Gamma M_S \gamma\rangle$ basis can be expressed in terms of the one-electron spin-orbit constants ζ_{tt} and ζ_{te} defined by¹

$$\zeta_{tt} = -2i \langle \xi^+ | t_z \cdot s_z | \eta^+ \rangle, \quad (5)$$

$$\zeta_{te} = -i \langle \xi^+ | t_z \cdot s_z | \epsilon^+ \rangle. \quad (6)$$

The indices t and e in these constants stand for the $t_{2g}(\xi, \eta, \zeta)$ and the $e_g(\theta, \epsilon)$ symmetry species of the octahedral group. If the t_{2g} and e_g orbitals are pure metallic 3d atomic orbitals (AO's), as it is in the case in crystal-field theory, $\zeta_{tt} = \zeta_{te} = \zeta_{3d}$. In general, however, these functions are molecular orbitals expressible in the form¹⁷

$$t = N_t (d_t^{\text{MO}} - \lambda_\pi \chi_\pi), \quad (7)$$

$$e = N_e (d_e^{\text{MO}} - \lambda_s \chi_s - \lambda_\sigma \chi_\sigma), \quad (8)$$

where N_t and N_e are normalization constants, d_t^{MO} and d_e^{MO} 3d atomic functions, λ_s , λ_σ , and λ_π covalency pa-

rameters, and χ_s , χ_σ , and χ_π ligand symmetry-adapted functions:¹⁵

$$\begin{aligned}\chi_s(\varepsilon) &= \frac{1}{2}N(\sigma e_g)(s_1 - s_2 + s_4 - s_5), \\ \chi_\sigma(\varepsilon) &= \frac{1}{2}N(\sigma e_g)(x_1 - y_2 + x_4 - y_5), \\ \chi_\pi(\xi) &= \frac{1}{2}N(\pi t_{2g})(z_2 + y_3 - z_5 - y_6), \\ \chi_\pi(\eta) &= \frac{1}{2}N(\pi t_{2g})(z_1 + x_3 - z_4 - x_6), \\ \chi_\pi(\zeta) &= \frac{1}{2}N(\pi t_{2g})(y_1 + x_2 - y_4 - x_5).\end{aligned}\quad (9)$$

The normalization constants $N(\sigma e_g)$, $N(\sigma e_g)$, and $N(\pi t_{2g})$ differ from unity by contributions from ligand-ligand overlaps. Notation in Eq. (9) follows the coordinate system of Ref. 15 depicted in Fig. 1.

Equations (7) and (8) resemble the traditional minimal-basis description of the valence MO's (Ref. 17). In this description d_t^{MO} and d_e^{MO} coincide with the free-ion $3d$ AO. However, Eqs. (7) and (8) become general if the d_t^{MO} and d_e^{MO} functions are allowed to have different radial parts (and different from the free-ion $3d$ AO) and χ_s , χ_σ , and χ_π differ from the pure-ligand functions. In particular, these equations are compatible with SCF calculations performed within a valence space containing an arbitrary number of basis functions. In this case, it is always possible to transform the actual MO's into the forms of Eqs. (7) and (8), as we show for the $3d$ case in the Appendix.

The important point here is to notice that the d_t^{MO} and d_e^{MO} functions are obtained from a cluster SCF calculation followed by the MO transformation discussed in the Appendix. In the calculations reported here we use a valence space with two $3d$ functions. The first one, $3d_M$, is the 2ξ Slater-type (STO) function of Richardson *et al.*¹⁸ The second function is the innermost STO of $3d_M$. Our SCF calculations give d_t^{MO} and d_e^{MO} functions with different radial forms. They are also different from

the $3d_M$ AO. As we will see, this $3d$ -orbital deformation produced by the SCF process has significant effects on the spin-orbit constants, as discussed by Marshall and Stuart.⁵

The orbital deformation has been traditionally described by means of a radial scaling of the free-ion AO. This means that the changes produced in this AO during the formation of the cluster can be collected in a single parameter *per* MO. The description given here through the d_t^{MO} and d_e^{MO} functions is much more general, being limited only by the flexibility of the SCF process. However, if the orbital deformation is not too large, as it has been the case in our calculations, the d_t^{MO} and d_e^{MO} functions can be regarded as radially scaled versions of the free-ion AO. In our basis

$$R(d_t^{\text{MO}}) = 3d_M(\lambda r), \quad (10)$$

$$R(d_e^{\text{MO}}) = 3d_M(\mu r), \quad (11)$$

where $R(d_t^{\text{MO}})$ and $R(d_e^{\text{MO}})$ are the radial parts of the d_t^{MO} and d_e^{MO} functions, respectively. The scaling factors λ and μ can be related to the nephelauxetic parameters discussed by Jorgensen.⁶ Once the d_t^{MO} and d_e^{MO} functions have been determined, λ and μ can be obtained by maximizing the $\langle R(d_t^{\text{MO}}) | 3d_M(\lambda r) \rangle$ and $\langle R(d_e^{\text{MO}}) | 3d_M(\mu r) \rangle$ overlap integrals, as discussed in the Appendix. This procedure gives scaled functions having minimum square deviation with respect to the $R(d^{\text{MO}})$ functions, i.e., it gives scaling factors consistent with the $R(d^{\text{MO}})$ function as a whole. Other criteria leading to a better simulation of specific parts of the given wave function may be preferred, depending on the wanted applications. Scaling parameters smaller (greater) than unity represent an expansion (contraction) of the $3d_M$ AO. We also relate these parameters to the spin-orbit constants below.

The spin-orbit coupling constants ζ_{tt} and ζ_{te} can be expressed as combinations of basic spin-orbit integrals by substituting Eqs. (7)–(9) into Eqs. (5) and (6). Misetic and Watson⁹ have shown that all two-center integrals appearing in such expression are negligible (they are all smaller than 1 cm^{-1}) due to the highly localized character of the $\xi^M(r_i)$ and $\xi^L(r_{ki})$ functions around their respective nuclei. Taking into account this result we can write¹

$$\zeta_{tt} = N_t^2 [\zeta_{d_{tt}} + \frac{1}{2} \lambda^2 \pi N(\pi t_{2g})^2 \zeta_L], \quad (12)$$

$$\zeta_{te} = N_t N_e [\zeta_{d_{te}} - \frac{1}{2} \lambda_\sigma \lambda_\pi N(\sigma e_g) N(\pi t_{2g}) \zeta_L]. \quad (13)$$

These have been the equations adopted in this work to compute the spin-orbit constants of the ML_6 cluster. They clearly show the two main factors affecting the final values of these constants, namely, (a) the metal-ligand covalency, explicitly appearing here in the form of the familiar λ_σ and λ_π parameters but also indirectly affecting the spin-orbit constants through the normalization constants N_t and N_e ; (b) the $3d$ -orbital deformation, appearing into the atomic parameter $\zeta_{d_{tt}}$ and $\zeta_{d_{te}}$.

We will detail now the calculation of these atomic pa-

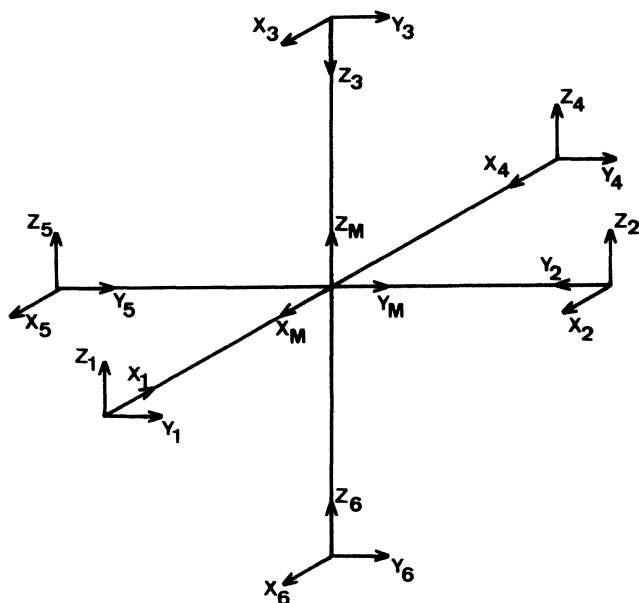


FIG. 1. Definition of the coordinate system.

rameters. In principle, they are given by the radial integrals:

$$\zeta d_{it} = \langle d_i^{\text{MO}} | \xi^M(r) | d_i^{\text{MO}} \rangle, \quad (14)$$

$$\zeta d_{ie} = \langle d_i^{\text{MO}} | \xi^M(r) | d_e^{\text{MO}} \rangle, \quad (15)$$

$$\zeta_L = \langle 2p_L | \xi^L(r_L) | 2p_L \rangle. \quad (16)$$

In this work, however, we compute them by means of a procedure that incorporates (a) the accurate atomic theory of the spin-orbit interaction developed by Blume and Watson,^{12,13} and (b) the results of our SCF calculations which provide a measure of the 3d-orbital deformation by giving the d_i^{MO} and d_e^{MO} functions.

The calculation is made in two steps.

(i) We compute theoretical spin-orbit parameters $\zeta^{\text{theor}}(d^{n-SL})$ associated to the free-ion d^{n-SL} multiplet, by means of the rigorous expressions given by Blume and

Watson¹² and the Horie coefficients¹⁹ which include the specific 3d-3d interactions for a given multiplet. For the d^3 , d^4 , and d^5 cases considered in this work, these theoretical parameters become^{20,21}

$$\zeta^{\text{theor}}(d^{3-4F}) = \zeta_c - (114/7)M^0(3d, 3d) - \frac{18}{49}M^2(3d, 3d), \quad (17)$$

$$\zeta^{\text{theor}}(d^{4-5D}) = \zeta_c - 24M^0(3d, 3d) + \frac{12}{7}M^2(3d, 3d), \quad (18)$$

$$\zeta^{\text{theor}}(d^{5-6S}) = \zeta_c - 7M^0(3d, 3d) + \frac{6}{7}M^2(3d, 3d). \quad (19)$$

The spin-orbit constant ζ_c , which contains the effects of the bare nucleus and the interaction of the 3d orbitals with the closed shells, is given by¹²

$$\begin{aligned} \zeta_c = & \frac{1}{2}Z\alpha^2 \langle r^{-3} \rangle_{3d} - \sum_{n=1}^3 [4M^0(3d, ns) - \frac{6}{5}V^1(3d, ns) - \frac{12}{5}N^2(3d, ns) + \frac{18}{5}N^0(3d, ns)] \\ & - \sum_{n=2}^3 [12M^0(3d, np) - \frac{6}{5}V^0(3d, np) - \frac{72}{35}V^2(3d, np) - \frac{72}{35}N^3(3d, np) - \frac{6}{7}N^1(3d, np) + \frac{24}{5}N^{-1}(3d, np)]. \end{aligned} \quad (20)$$

The M^k , N^k , and V^k radial integrals in Eqs. (17)–(20) are given by¹²

$$M^k(ab) = (\alpha^2/4) \int r_1^2 r_2^2 R_a^2(r_1) R_b^2(r_2) (r_2^k / r_1^{k+3}) \epsilon(r_1 - r_2) dr_1 dr_2, \quad (21)$$

$$N^k(ab) = (\alpha^2/4) \int r_1^2 r_2^2 R_a(r_1) R_b(r_2) R_a(r_2) R_b(r_1) (r_2^k / r_1^{k+3}) \epsilon(r_1 - r_2) dr_1 dr_2, \quad (22)$$

$$V^k(ab) = (\alpha^2/4) \int r_1^2 r_2^2 R_a(r_1) R_b(r_2) (r_2^k / r_1^{k+3}) (r_2 \partial / \partial r_1 - r_1 \partial / \partial r_2) R_a(r_2) R_b(r_1) dr_1 dr_2. \quad (23)$$

In these formulas $\epsilon(r_1 - r_2) = 1$ if $r_1 > r_2$ and it is zero if $r_1 < r_2$. Using Eqs. (17)–(23) and the basis sets adopted in this work^{18,22} we obtained the atomic parameters $\zeta^{\text{theor}}(d^{n-SL})$ collected in Table I.

(ii) The ζd_{it} and ζd_{ie} spin-orbit coupling parameters are computed with the formulas in Eqs. (17)–(19), but using the d_i^{MO} and d_e^{MO} functions obtained from the cluster SCF calculations instead of the free-ion 3d AO. In this way, we introduce ‘‘octahedral’’ spin-orbit constants with t_{2g} or e_g character and incorporate in these parameters the desired 3d-orbital deformation. To recall the use of this different basis set and the octahedral character of the

new parameters we will denote them as $\zeta d_{it}^{\text{theor}}(t_{2g}^x e_g^y - S\Gamma)$ and $\zeta d_{ie}^{\text{theor}}(t_{2g}^x e_g^y - S\Gamma)$, the parentheses making reference to the cluster electronic state in which the SCF equations have been solved. Recall that in spite of this molecular-looking notation these are still one-center parameters.

The use of the d_i^{MO} and d_e^{MO} functions in Eqs. (17)–(19) deserves a few comments. First, we have to compute ζ_c using Eq. (20). In order to compute the $\zeta d_{it}^{\text{theor}}(t_{2g}^x e_g^y - S\Gamma)$ constant we introduce d_i^{MO} and find a value that can be called $\zeta_c(tt)$. To obtain $\zeta d_{ie}^{\text{theor}}(t_{2g}^x e_g^y - S\Gamma)$ we require d_i^{MO} and d_e^{MO} , as it would be the case if were using Eq. (15), and find a value that can analogously

TABLE I. Experimental and theoretical spin-orbit parameters (cm^{-1}) for the V^{2+} , Cr^{z+} ($z = 1-3$), and Mn^{2+} ions.

Ion	Config.	Term	$\zeta^{\text{theor}}(d^{n-SL})^a$	$\zeta^{\text{expt b}}$	$k = \zeta^{\text{expt}} / \zeta^{\text{theor}}(d^{n-SL})$
V^{2+}	$3d^3$	$4F$	170	168	0.9882
Cr^+	$3d^5$	$6S$	212	212 ^c	1.0000
Cr^{2+}	$3d^4$	$3D$	218	232	1.0642
Cr^{3+}	$3d^3$	$4F$	252	276	1.0952
Mn^{2+}	$3d^5$	$6S$	307	327 ^d	1.0651

^aComputed with Eqs. (17)–(19) and basis sets from Ref. 18.

^bReference 20.

^cReference 37.

^dReference 38.

be called $\zeta_c(te)$. However, the presence of two different radial deformations in the d^{MO} basis, corresponding to the t_{2g} and e_g symmetries, would require a detailed discussion related to the calculation of the $3d$ - $3d$ two-electron integrals in Eqs. (17)–(19). We avoid such complexity by computing these interactions with the free-ion basis sets. This approximation does not introduce appreciable errors at all because, on the one hand, the $3d$ deformation is not large and, on the other hand, these $3d$ - $3d$ interactions are a very small part of the total $\zeta^{\text{theor}}(d^n, SL)$ parameter. Thus the quantities $\zeta d^{\text{theor}}(t_{2g}^x e_g^y, S\Gamma)$ computed with Eqs. (17)–(19) contain the same $3d$ - $3d$ interaction as the $\zeta^{\text{theor}}(d^n, SL)$ ones but they differ from the latter in that ζ_c is $\zeta_c(tt)$ in $\zeta d_{tt}^{\text{theor}}(t_{2g}^x e_g^y, S\Gamma)$ and $\zeta_c(te)$ in $\zeta d_{te}^{\text{theor}}(t_{2g}^x e_g^y, S\Gamma)$.

The ζd_{tt} and ζd_{te} parameters computed in this way can still be improved by correcting them from the errors introduced in the free-ion calculation. Such correction may be easily incorporated if we first obtain the empirical ratio $k = \zeta^{\text{exp}}/\zeta^{\text{theor}}(d^n, SL)$, where ζ^{exp} is the observed free-ion coupling constant, and then write

$$\zeta d_{tt} = k \zeta d_{tt}^{\text{theor}}(t_{2g}^x e_g^y, S\Gamma), \quad (24)$$

$$\zeta d_{te} = k \zeta d_{te}^{\text{theor}}(t_{2g}^x e_g^y, S\Gamma). \quad (25)$$

Values for these empirical ratios have been collected in Table I.

Equations (24) and (25) are the final forms we used to obtain the ζd_{tt} and ζd_{te} parameters required in Eqs. (12) and (13). Notice that these quantities will depend on the metal-ligand distance R because the $3d$ -orbital deformation included in the d_t^{MO} and d_e^{MO} functions and estimated by means of cluster SCF calculations should change with R .

The ligand parameter ζ_L cannot be computed in the same way as ζd_{tt} and ζd_{te} in Eqs. (24) and (25) because there is not an experimental free-ion value to determine the ratio k . The theoretical parameter computed with the basis set of Clementi and Roetti²³ turns out to be 224 cm^{-1} . Missetich and Buch⁸ and Missetich and Watson⁹ adopted a free-ion value of 220 cm^{-1} found by extrapolation from observed and calculated data for the sequence F^{3+} , F^{2+} , F^+ , and neutral F . On the other hand, Eqs. (12) and (13) show that the contribution of ζ_L to the final spin-orbit constants includes as a factor half the square of a covalency parameter. Since these parameters are hardly larger than 0.35 in the fluorides analyzed here, we see that ζ_L will be multiplied by a factor smaller than 0.08 in these equations. In the much more covalent $\text{Cu}^{2+}:\text{ZnS}$ and $\text{Cu}^{2+}:\text{CdS}$ systems Setyono and Scherz¹¹ found that the contribution of ζ_L to the final constant is 7%. Thus uncertainties in the estimation of ζ_L , including radial expansion effects, would represent, at most, 1 or 2 cm^{-1} in the final value of the total spin-orbit constant. It seems then worthless to explore such effects in ζ_L . Accordingly, we have adopted the criterion in Refs. 8 and 9 and have used in this work the extrapolated value $\zeta_L = 220 \text{ cm}^{-1}$.

HARTREE-FOCK RESULTS AND DISCUSSION

The open-shell Hartree-Fock-Roothaan methodology of Richardson *et al.*¹⁵ has been used to compute the electronic structure of the $(\text{CrF}_6)^{n-}$ ($n = 3-5$), $(\text{MnF}_6)^{4-}$, and $(\text{VF}_6)^{4-}$ systems in KMgF_3 , at several values of the metal-ligand distance R . The metallic basis sets have been taken from Refs. 18 and 22, and the fluoride basis from Ref. 10. These bases are formed of Slater-type orbitals (STO). The frozen-core approximation¹⁵ has been adopted in the calculation, the valence shell being formed by the $3s$, $3p$, $3d$, $3d'$, $4s$, and $4p$ metallic AO's plus the $2s$ and $2p$ AO's of the six fluoride ions. As commented above, the $3d$ AO is a 2ζ function and $3d'$ its innermost STO. Insufficient core-valence orthogonality usually occurring in frozen-core calculations has been corrected by means of core-projection operators as described in Refs. 24 and 25. All ligand-ligand integrals have been accurately computed by following the renormalization procedure described by Kalman and Richardson.²⁶ The cluster-lattice interaction has been introduced by means of an accurate lattice potential (as described in Ref. 29). This potential is made of the nuclear and electronic contributions of the lattice ions. The orthogonality between the cluster wave functions and the AO's of the lattice ions is enforced by means of adequate lattice projection operators.²⁷ This lattice effective potential is included in the Fock operator of the cluster before the SCF process. In this way, the resulting cluster MO's are consistent with the external environment.

These SCF calculations lead to the determination of the ground-state nuclear potentials, along the totally symmetry vibration of the cluster, and then to the equilibrium metal-ligand distance R_e . These values of R_e 's are collected in Table II. They differ from the values determined by x-ray diffraction or by analysis of the observed isotropic superhyperfine constant A_s (Ref. 28) by a few hundredths of an Å (Ref. 29).

Covalency parameters λ_σ and λ_π and normalization constants N_t and N_e , required for the calculation of the ζ_{tt} and ζ_{te} parameters, have been deduced from the canonical MO's, as discussed in the Appendix. For the d^3 systems $(\text{CrF}_6)^{3-}$ and $(\text{VF}_6)^{4-}$, having empty the mainly metal, antibonding e_g MO, the covalency parameters and normalization constants have been estimated from the "average" $t_{2g}^2 e_g^{-4} T_{\text{av}}$ state with an electronic energy equal to the average energy of the ${}^4T_{1g}$ and ${}^4T_{2g}$ states of this configuration. In these cases, the ground-

TABLE II. Theoretical values of the metal-fluoride equilibrium distance R_e (Å) for octahedral $(MF_6)^{n-}$ ions. $M = \text{V}^{2+}$, Cr^{2+} ($z = 1-3$), and Mn^{2+} .

System	Configuration	Multiplet	R_e
$\text{V}^{2+}:\text{KMgF}_3$	$t_{2g}(3)$	${}^4A_{2g}$	2.055
$\text{Cr}^+:\text{KMgF}_3$	$t_{2g}(3)e_g(2)$	${}^6A_{1g}$	2.195
$\text{Cr}^{2+}:\text{KMgF}_3$	$t_{2g}(3)e_g(1)$	5E_g	2.056
$\text{Cr}^{3+}:\text{KMgF}_3$	$t_{2g}(3)$	${}^4A_{2g}$	1.897
$\text{Mn}^{2+}:\text{KMgF}_3$	$t_{2g}(3)e_g(2)$	${}^6A_{1g}$	2.066

state equilibrium distance is computed from the SCF solutions of the $t_{2g}^3 e_g^{-4} A_{2g}$ state and the optical spectrum, including the spin-orbit constant, from the SCF solutions of the $t_{2g}^2 e_g^{-4} T_{av}$ state.

Let us examine now the numerical results. First, we will comment on the effects of the $3d$ -orbital deformation on the spin-orbit constants. In Table III we collect the atomic parameters ζd_{it} and ζd_{ie} [Eqs. (24) and (25)] computed with $k=1$ at several values of R . For the five systems investigated here we see that ζd_{it} is smaller than the free-ion value and tends to such limit at larger distances. On the contrary, ζd_{ie} turns out to be nearly independent of R ; it is also smaller than the free-ion value but greater than ζd_{it} .

The behavior of these parameters correlates with the $3d$ -orbital deformation, as measured by the scaling parameters of Eqs. (10) and (11). These parameters appear in Table IV. First, it may be interesting to remark that scaling parameters obtained by simulating the $\langle r^{-n} \rangle$ expectation values differ very slightly from those collected in Table IV. For instance, in this table we read a value of $\lambda=0.9803$ for $Mn^{2+}:KMgF_3$ at $R=4.00$ a.u. This parameter turns out to be 0.9787 and 0.9827 for $n=1$ and 3, respectively.

Numbers in Table IV reveal that the d_{it}^{MO} orbital significantly expands with respect to the free-ion $3d$ AO. This effect increases when R decreases. However, the deformation experienced by the d_{ie}^{MO} function is much smaller. It is also different for different distances: this function slightly expands at larger distances (the Mn^{2+} ion is an exception) but it suffers a contraction at shorter distances.

In agreement with the arguments by Marshall and Stuart,⁵ the scaling parameter $\lambda < 1$ correlates with a reduction of the ζd_{it} parameter. Also, the larger expansions of the d_{it}^{MO} functions are consistent with ζd_{it} values smaller than the ζd_{ie} ones.

At this point it is interesting to remark that the relations

$$\zeta d_{it}^{\text{theor}}(t_{2g}^x e_g^y {}^S\Gamma) = \lambda^3 \zeta^{\text{theor}}(d^{n-S}L), \quad (26)$$

$$\zeta d_{ie}^{\text{theor}}(t_{2g}^x e_g^y {}^S\Gamma) = (\lambda\mu)^{3/2} \zeta^{\text{theor}}(d^{n-S}L), \quad (27)$$

which would hold if $\zeta d_{it}^{\text{theor}}(t_{2g}^x e_g^y {}^S\Gamma)$ and $\zeta d_{ie}^{\text{theor}}(t_{2g}^x e_g^y {}^S\Gamma)$ were proportional to $\langle r^{-3} \rangle_{3d}$ (Ref. 5), are very well satisfied in the present calculation. In Table V we collect the values of $\zeta d_{it}^{\text{theor}}(t_{2g}^3 e_g^{2,6} A_{1g})$ and $\zeta d_{ie}^{\text{theor}}(t_{2g}^3 e_g^{2,6} A_{1g})$ for the $(MnF_6)^{4-}$ ion computed by means of Eqs. (26) and (27). Deviations from the values in Table III are in all cases smaller than 3 cm^{-1} and decrease at large distances. From this result we can conclude that the present $3d$ deformation may be fully captured by the scaling approximation. Our numbers suggest that this is so because this deformation is essentially produced by changes in the first term of ζ_c . This term has the form considered by Marshall and Stuart.⁵ The modifications induced by the $3d$ deformation in the $3d$ -core interactions appearing in Eq. (20) are negligible.

In applying Eq. (20) we have assigned a population of $2(2l+1)$ electrons to the closed-shell orbitals. In our frozen-core calculation this is totally correct for all but the $3s$ and $3p$ functions forming part of the valence shell. The two electrons occupying the mainly $3s$ MO do not

TABLE III. ζd_{it} (first row) and ζd_{ie} (second row) spin-orbit parameters (cm^{-1}) for the $V^{2+}:KMgF_3$, $Cr^{2+}:KMgF_3$ ($z=1-3$), and $Mn^{2+}:KMgF_3$ systems computed by means of Eqs. (24) and (25), and $k=1$.

R (a.u.)	$Cr^{+}:KMgF_3$	$Cr^{2+}:KMgF_3$	$Cr^{3+}:KMgF_3$	R (a.u.)	$V^{2+}:KMgF_3$	$Mn^{2+}:KMgF_3$
3.05			208.1	3.00	113.7	249.2
			236.6		153.9	292.2
3.15			213.1	3.20	125.0	264.6
			237.0		152.7	294.4
3.26	152.9	179.6	217.5	3.40	132.7	274.7
	191.4	204.8	237.6		153.1	296.9
3.425	162.1	185.6	222.2	3.60	138.1	281.5
	192.2	205.2	238.7		153.9	298.9
3.59	169.2	190.1	225.4	3.80	141.9	286.2
	193.3	205.9	239.4		154.6	300.3
3.772		193.7		4.00	144.7	289.6
		206.5			155.1	301.1
3.99	180.4	196.8	229.5	4.20	146.8	292.1
	195.8	206.8	239.8		155.4	301.4
4.19	184.2	198.9		4.40	148.4	294.0
	196.6	206.9			155.4	301.5
4.39	187.1	200.6	230.9			
	197.1	206.8	238.4			
4.59	189.3					
	197.3					
4.99	192.2					
	197.3					
∞	211.5	218.1	251.7	∞	169.6	307.2
	211.5	218.1	251.7		169.6	307.2

TABLE IV. Scaling factors corresponding to the d_t^{MO} (first row) and d_e^{MO} (second row) functions.

R (a.u.)	$\text{Cr}^+:\text{KMgF}_3$	$\text{Cr}^{2+}:\text{KMgF}_3$	$\text{Cr}^{3+}:\text{KMgF}_3$	R (a.u.)	$\text{V}^{2+}:\text{KMgF}_3$	$\text{Mn}^{2+}:\text{KMgF}_3$
3.05			0.9439	3.00	0.9081	0.9358
			1.0217		1.0640	1.0397
3.15			0.9503	3.20	0.9264	0.9526
			1.0147		1.0277	1.0226
3.26	0.9213	0.9480	0.9558	3.40	0.9391	0.9638
	1.0383	1.0203	1.0098		1.0110	1.0151
3.425	0.9336	0.9561	0.9619	3.60	0.9479	0.9713
	1.0220	1.0115	1.0056		1.0027	1.0112
3.59	0.9429	0.9620	0.9660	3.80	0.9541	0.9765
	1.0124	1.0063	1.0030		0.9977	1.0086
3.772		0.9669		4.00	0.9587	0.9803
		1.0024			0.9941	1.0064
3.99	0.9580	0.9711	0.9713	4.20	0.9621	0.9831
	1.0009	0.9988	0.9980		0.9910	1.0042
4.19	0.9629	0.9739		4.40	0.9648	0.9852
	0.9974	0.9959			0.9882	1.0021
4.39	0.9668	0.9762	0.9730			
	0.9945	0.9933	0.9925			
4.59	0.9699					
	0.9919					
4.99	0.9738					
	0.9875					
∞	1.0000	1.0000	1.0000	∞	1.0000	1.0000
	1.0000	1.0000	1.0000		1.0000	1.0000

TABLE V. ζd_{ii} and ζd_{ie} spin-orbit parameters (cm^{-1}) for the Mn^{2+} ion as computed with Eqs. (26) and (27).

R (a.u.):	3.00	3.20	3.40	3.60	3.80	4.00	4.20	4.40
ζd_{ii} :	251.7	265.6	275.0	281.5	286.1	289.4	291.9	293.8
ζd_{ie} :	294.8	295.4	297.3	299.0	300.3	301.0	301.3	301.4

TABLE VI. ζ_{ii} (first row) and ζ_{ie} (second row) spin-orbit constants (cm^{-1}) for the $\text{V}^{2+}:\text{KMgF}_3$, $\text{Cr}^{z+}:\text{KMgF}_3$ ($z = 1-3$), and $\text{Mn}^{2+}:\text{KMgF}_3$ systems.

R (a.u.)	$\text{Cr}^+:\text{KMgF}_3$	$\text{Cr}^{2+}:\text{KMgF}_3$	$\text{Cr}^{3+}:\text{KMgF}_3$	R (a.u.)	$\text{V}^{2+}:\text{KMgF}_3$	$\text{Mn}^{2+}:\text{KMgF}_3$
3.05			241.5	3.00	138.9	286.1
			242.7		146.8	315.1
3.15			243.6	3.20	141.7	294.2
			241.6		144.4	313.1
3.26	172.7	204.0	245.4	3.40	143.4	299.6
	196.5	213.9	241.0		143.9	312.7
3.425	176.3	206.3	247.4	3.60	144.6	303.6
	195.3	213.1	240.8		144.3	313.1
3.59	179.2	208.1	248.9	3.80	145.5	306.8
	194.8	213.0	240.8		145.0	313.7
3.772		209.7		4.00	146.3	309.3
		213.2			145.8	314.3
3.99	184.5	211.4	251.2	4.20	147.1	311.5
	195.0	214.3	240.8		146.6	315.0
4.19	186.7	212.8		4.40	147.9	313.2
	195.3	213.9			147.3	315.7
4.39	188.6	214.2	252.3			
	195.5	214.3	239.9			
4.59	190.3					
	195.8					
4.99	192.6					
	195.9					
∞	212	232	276	∞	168	327
	212	232	276		168	327

belong completely to the metal 3s AO, as well as the six electrons of the mainly 3p MO do not belong entirely to the 3p AO. Nevertheless, the distortion of these closed-shell AO's is very small and the electron assignment we have made does not introduce any appreciable change in the values of the spin-orbit parameters.

Let us see now the effects of the metal-ligand covalency on the spin-orbit constants. To appreciate this effect we will compare the $\zeta_{d_{tt}}$ and $\zeta_{d_{te}}$ parameters presented above with the constants computed by means of Eqs. (12) and (13). In using these equations we have computed the metallic parameters $\zeta_{d_{tt}}$ and $\zeta_{d_{te}}$ from Eqs. (24) and (25) with the values of the empirical ratio k collected in Table I. The resulting ζ_{tt} and ζ_{te} constants appear in Table VI. From the numbers in this table we deduce several conclusions.

First, in agreement with Marshall and Stuart,⁵ the ζ_{tt} constants increase for increasing covalency, the effect being larger at shorter distances. This spin-orbit constant increases with R , as the $\zeta_{d_{tt}}$ parameter does, although the increasing ratio is greater for the latter, as can be seen in Fig. 2. This figure reveals two significant results: (a) the 3d deformation effect is important even at larger distances, given the existing difference between $\zeta_{d_{tt}}(R)$ and the free-ion values ($R = \infty$) and (b) the effects of the covalency disappear at relatively short distances, as indicated by the merging of the $\zeta_{d_{tt}}(R)$ and $\zeta_{tt}(R)$ curves. Thus, as expected, the covalency behaves as a quantum-mechanical short-ranged interaction.

In Fig. 3 we can see analogous $\zeta_{te}(R)$ and $\zeta_{d_{te}}(R)$ plots. It is noticeable the near- R independence of these "symmetry-mixed" spin-orbit parameters. A second difference with the $t_{2g}-t_{2g}$ parameters is that here the covalency tends to reduce the values of the spin-orbit constants, with the exceptions of $\text{Mn}^{2+}:\text{KMgF}_3$ and $\text{Cr}^+:\text{KMgF}_3$ at very short distances. As a third difference we observe in this figure that the atomic and

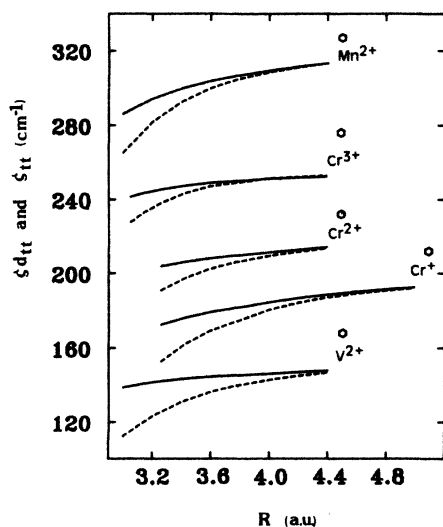


FIG. 2. R dependence of the ζ_{tt} (solid lines) and $\zeta_{d_{tt}}$ (dashed lines) spin-orbit coupling constants for the $\text{V}^{2+}:\text{KMgF}_3$, $\text{Cr}^{2+}:\text{KMgF}_3$ ($z=1-3$), and $\text{Mn}^{2+}:\text{KMgF}_3$ systems. Note. Free-ion values have been represented by hexagons.

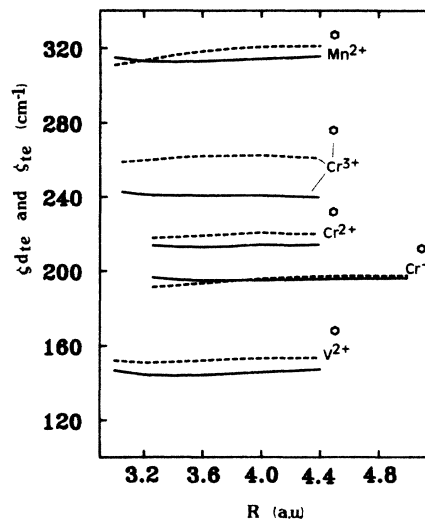


FIG. 3. R dependence of the ζ_{te} (solid lines) and $\zeta_{d_{te}}$ (dashed lines) spin-orbit couplings constants for the $\text{V}^{2+}:\text{KMgF}_3$, $\text{Cr}^{2+}:\text{KMgF}_3$ ($z=1-3$), and $\text{Mn}^{2+}:\text{KMgF}_3$ systems. Note. Free-ion values have been represented by hexagons.

cluster parameters do not merge in the range of R examined. This behavior seems to be related to the anomalous long-range R dependence of the λ_{σ} covalency parameter, a possible artifact of our SCF calculations.³⁰ We finally notice that, as it should be, the ζ_{tt} and ζ_{te} constants tend to coincide at large distance (Table VI), the $(\text{CrF}_6)^{3-}$ being the single exception. This exception might also be related to an anomalous prediction of the R dependence of the covalency in this system. A better description would require inclusion of configuration interaction involving charge-transfer states but we have not considered this refinement in this work.

Let us compare now the theoretical spin-orbit constants with the available experimental data. In Table VII we collect the constants computed at the theoretical equilibrium distance and their reduction with respect to the free-ion value. As commented above, accurate empirical data are scarce and some results may be in appreciable error.⁷

For the $(\text{MnF}_6)^{4-}$ ion we can compare our $\zeta_{tt}=308$ and $\zeta_{te}=314 \text{ cm}^{-1}$ with the 320 cm^{-1} given by Mehra and Venkateswarlu³¹ for RbMnF_3 . Although these numbers are not immediately comparable, given the different crystal lattice and equilibrium distance, the agreement is reasonable. Our result agrees well with the semiempirical one given by Cole and Garrett,⁷ 304 cm^{-1} , for Mn^{2+} in RbMnF_3 and KMnF_3 .

For the $(\text{VF}_6)^{4-}$ ion Sturge *et al.*³ estimated the spin-orbit constant from values of $10Dq$, the angular momentum reduction factor $k_{\sigma\pi}$, and the g factor. Using the approximate equation

$$g = 2.0023 - (8/3)k_{\sigma\pi}\zeta_{te}/10Dq \quad (28)$$

and taking $g=1.9720$, $10Dq=12000 \text{ cm}^{-1}$, and $k_{\sigma\pi}=0.96$, they find $\zeta_{te}=142 \text{ cm}^{-1}$, in very remarkable agreement with our 145 cm^{-1} in Table VII.

TABLE VII. ζ_{ii} and ζ_{ie} spin-orbit constants (cm^{-1}) and their reduction (%) with respect to the corresponding free-ion values, as computed at the theoretical equilibrium geometry of the $M^{z+}:\text{KMgF}_3$ systems. $M = \text{V}^{2+}$, Cr^{2+} ($z = 1-3$), and Mn^{2+} .

	$\text{Cr}^{+}:\text{KMgF}_3$	$\text{Cr}^{2+}:\text{KMgF}_3$	$\text{Cr}^{3+}:\text{KMgF}_3$	$\text{V}^{2+}:\text{KMgF}_3$	$\text{Mn}^{2+}:\text{KMgF}_3$
ζ_{ii}	186	211	249	146	308
Reduction	12	9	10	13	6
ζ_{ie}	195	214	241	145	314
Reduction	8	8	10	13	4
B^a	681	750	808	697	885
C^a	2427	3057	3336	2676	3059

^a B and C electron-repulsion parameters (cm^{-1}), taken from Ref. 34, have been computed through cluster-*in-vacuo* calculations.

For the $(\text{CrF}_6)^{4-}$ and $(\text{CrF}_6)^{5-}$ ions we do not find any empirical estimation of the spin-orbit coupling constant. For $(\text{CrF}_6)^{3-}$, our calculation gives values about 10% larger than those reported by Wong *et al.*³² for $\text{Cr}^{3+}:\text{K}_2\text{NaGaF}_6$, 225 cm^{-1} , and Ferguson *et al.*³³ for K_2NaCrF_6 , 227 cm^{-1} .

To conclude the discussion we would like to refer to the linear correlations between spin-orbit constants and electron-repulsion parameters discussed by Cole and Garrett⁷ in their study of the spin-orbit interaction in transition-metal compounds. It seems natural to ask whether these correlations appear or not within the theoretically calculated quantities. Theoretical electron-repulsion Racah parameters for the octahedral clusters analyzed here were computed by Francisco *et al.*³⁴ They are included in Table VII. In Ref. 34 the electronic energies of all the d^n states were first computed, by means of the frozen-orbital approximation, from the SCF solution of the ground state. The ${}^4T_{av}$ state introduced above were used for the d^3 systems. The Tanabe-Sugano matrices¹ were then fitted to these theoretical electronic transitions through a linearization procedure.³⁵ Thus, for a given cluster, the spin-orbit constants of this paper and the electron-repulsion parameters of Ref. 34 come from the solution of the same electronic state. The electron-repulsion parameters, however, were obtained from cluster-*in vacuo* results. Given the uniformly small effects of the cluster-lattice interaction on the $d-d$ transitions, as computed in Ref. 36, we think that the following comparison and qualitative conclusions deduced from Table VII would be reasonably consistent.

From this table we see very clear qualitative correlations for the isovalent sequence: V^{2+} , Cr^{2+} , Mn^{2+} , the isometallic series: Cr^+ , Cr^{2+} , Cr^{3+} , and the isoelectronic pairs V^{2+} , Cr^{3+} , and Cr^+ , Mn^{2+} . In the isoelectronic and isovalent sequences both Racah parameters and spin-orbit constants increase with the nuclear charge, and in the isometallic series these parameters increase with increasing ionization. Clearly, these few examples do not allow for generalizations but these qualitative trends hold quite well.

On the other hand, the work by Flórez *et al.*³⁶ shows that for the $(\text{MnF}_6)^{4-}$ cluster the theoretical B and C parameters are fairly independent of the metal-ligand distance. This behavior contrasts with the clear R dependence of ζ_{ii} shown in Fig. 2, but it is consistent with the

near independence of R shown by ζ_{ie} (Fig. 3). Such result may be understood if we recall that the theoretical B and C parameters are obtained through a process that mixes $t_{2g}-t_{2g}$, $t_{2g}-e_g$, and e_g-e_g electron-repulsion interactions.³⁵ In conclusion, our results suggest that the theoretical spin-orbit constants might well correlate with theoretical electron-repulsion parameters through isovalent, isometallic, and isoelectronic sequences. For a given cluster, the R dependence of the electron-repulsion parameters would more resemble the behavior of ζ_{ie} than that of ζ_{ii} .

CONCLUSIONS

We have used the Hamiltonian of Misetich and Buch⁸ in combination with Hartree-Fock-Roothaan calculations to compute crystal spin-orbit parameters and examine the effects of $3d$ -orbital expansion and metal-ligand covalency on these quantities. The V^{2+} , Cr^{2+} ($z = 1-3$), and Mn^{2+} ions in KMgF_3 have been studied. The modifications of the spin-orbit radial functions induced by bonding effects have been obtained from the SCF results by means of a procedure that permits an easy transference of any theoretical refinement in the cluster calculation into the computed spin-orbit constants. However, the ligand constant ζ_L has been taken from earlier estimations because the equations of the Misetich and Buch formalism⁸ reveal that the uncertainties in this parameter have a negligible effect on the final spin-orbit constant.

Our calculations show that the $3d$ -orbital deformation plays a significant role in determining the final value of the spin-orbit constants. We have considered only two $3d$ functions in the valence space but this small extension of the number of $3d$ functions is enough to show the importance of the mechanism advanced by Marshall and Stuart.⁵

The metal-ligand covalency turns out to have a minor contribution to the spin-orbit constants considered in this work. This picture may be different in more covalent systems such as oxides and chlorides.

The ligand contributions are also small, never larger than 10% of the final constants. Analogous results were found by Setyono and Scherz¹¹ for Cu^{2+} in ZnS and CdS .

The theoretical spin-orbit constants show the reduction

from the free-ion values detected in the empirically determined quantities. This reduction is essentially produced by the 3d-orbital expansion. The variation of this expansion with the metal-ligand distance is presented and discussed in this paper.

The work by Florez *et al.* has shown that the lattice effects have a minor influence into the covalency parameters³⁰ and nephelauxetic ratios³⁶ determining the crystal spin-orbit constants. Due to this, the results presented here may apply to other 3d fluorides as well.

Finally, the method proposed in this work gives theoretical spin-orbit coupling constants in rather good agreement with available experimental data. Thus, it appears that these theoretical constants would be accurate enough to be used with confidence in the study of the optical and electron resonance spectra of 3d ions in fluorides.

ACKNOWLEDGMENTS

One of us (E.F.) wants to thank the Ministerio de Educación y Ciencia of Spain for support. Financial support from Comisión Asesora de Investigación Científica y Técnica, Project No. 2880/83, is gratefully acknowledged.

APPENDIX

We proceed to prove that Eqs. (7) and (8) are compatible with SCF results obtained within an extended 3d basis set. The valence MO's deduced from such SCF calculations will have the form

$$t = \sum_{k=1}^M c_k \psi_{3d}(k) + c_\pi \chi_\pi, \quad (\text{A1})$$

$$e = \sum_{k=1}^M d_k \psi_{3d}(k) + c_s \chi_s + c_\sigma \chi_\sigma, \quad (\text{A2})$$

being c_k , d_k , c_π , c_s , and c_σ the SCF coefficients, and M the number of 3d functions used in the SCF calculation. If these 3d functions are in turn expressed in terms of N basis functions f_i :

$$\psi_{3d}(k) = \sum_{i=1}^N a_{ik} f_i. \quad (\text{A3})$$

Equations (A1) and (A2) become

$$t = \sum_{i=1}^N \sum_{k=1}^M c_k a_{ik} f_i + c_\pi \chi_\pi, \quad (\text{A4})$$

$$e = \sum_{i=1}^N \sum_{k=1}^M d_k a_{ik} f_i + c_s \chi_s + c_\sigma \chi_\sigma. \quad (\text{A5})$$

The 3d part of each of these MO's can be written as a new 3d function expanded over the same basis set, namely,

$$\sum_{i=1}^N \sum_{k=1}^M c_k a_{ik} f_i = \sum_{i=1}^N p_i f_i = N_t d_t^{\text{MO}}, \quad (\text{A6})$$

$$\sum_{i=1}^N \sum_{k=1}^M d_k a_{ik} f_i = \sum_{i=1}^N q_i f_i = N_e d_e^{\text{MO}}. \quad (\text{A7})$$

It is clear that the new d_t^{MO} and d_e^{MO} functions differ from the free-ion 3d AO because they depend upon the details of the particular cluster SCF calculation, through the c_k and d_k coefficients.

Normalization of the d_t^{MO} and d_e^{MO} functions gives

$$N_t = \left[\sum_{i,j}^N p_i p_j \langle f_i | f_j \rangle \right]^{1/2}, \quad (\text{A8})$$

$$N_e = \left[\sum_{i,j}^N q_i q_j \langle f_i | f_j \rangle \right]^{1/2}. \quad (\text{A9})$$

Introducing the d_t^{MO} and d_e^{MO} functions in Eqs. (A4) and (A5) we get the traditional single-3d-basis form of Eqs. (7) and (8):

$$t = N_t (d_t^{\text{MO}} + c_\pi N_t^{-1} \chi_\pi), \quad (\text{A10})$$

$$e = N_e (d_e^{\text{MO}} + c_s N_e^{-1} \chi_s + c_\sigma N_e^{-1} \chi_\sigma), \quad (\text{A11})$$

with

$$\lambda_\pi = -c_\pi N_t^{-1}, \quad (\text{A12})$$

$$\lambda_s = -c_s N_e^{-1}, \quad (\text{A13})$$

$$\lambda_\sigma = -c_\sigma N_e^{-1}. \quad (\text{A14})$$

The scaling factors appearing in Eqs. (10) and (11) can be computed as follows. Let, for instance, the 3d AO and the new d_t^{MO} functions be expanded over the basis set:

$$3d_M(r) = \sum_i^N m_i f_i, \quad (\text{A15})$$

$$d_t^{\text{MO}}(r) = \sum_i^N n_i f_i. \quad (\text{A16})$$

The scaled $3d_M(\lambda r)$ STO function can be written as

$$3d_M(\lambda r) = \lambda^{7/2} \sum_i^N m_i [(2\xi_i)^7 / 6!]^{1/2} r^2 \exp(-\lambda \xi_i r) \quad (\text{A17})$$

and the scale factor λ may be computed by maximizing the overlap integral:

$$\begin{aligned} \mathbf{S}(\lambda) &= \langle 3d_M(\lambda r) | d_t^{\text{MO}} \rangle \\ &= \lambda^{7/2} \sum_{i,j}^N h_{ij} (\lambda \xi_i + \xi_j)^{-7}, \end{aligned} \quad (\text{A18})$$

where $h_{ij} = 2^7 m_i n_j (\xi_i \xi_j)^{7/2}$.

The equation $\partial \mathbf{S}(\lambda) / \partial \lambda = 0$ is a polynomial in λ that can be solved iteratively by using the expression

$$\lambda = \left[\sum_{i,j}^N h_{ij} (\lambda \xi_i + \xi_j)^{-7} \right] \left[2 \sum_{i,j}^N h_{ij} \xi_i (\lambda \xi_i + \xi_j)^{-8} \right]^{-1}. \quad (\text{A19})$$

- ¹S. Sugano, Y. Tanabe, and H. Kamimura, *Multiplets of Transition-Metal Ions in Crystals* (Academic, New York, 1970).
- ²J. S. Griffith, *The Theory of Transition-Metal Ions* (Cambridge University Press, Cambridge, 1971).
- ³M. D. Sturge, F. R. Merrit, L. F. Johnson, H. J. Guggenheim, and J. P. Van der Ziel, *J. Chem. Phys.* **54**, 405 (1971).
- ⁴J. Owen, *Proc. R. Soc. London, Ser. A* **227**, 183 (1954).
- ⁵N. Marshall and R. Stuart, *Phys. Rev.* **123**, 2048 (1961).
- ⁶C. K. Jorgensen, *Modern Aspects of Ligand Field Theory* (North-Holland, Amsterdam, 1971), Chap. 23.
- ⁷G. M. Cole, Jr. and B. B. Garrett, *Inorg. Chem.* **9**, 1898 (1970).
- ⁸A. A. Missetich and T. Buch, *J. Chem. Phys.* **41**, 2524 (1964).
- ⁹A. A. Missetich and R. E. Watson, *Phys. Rev.* **143**, 335 (1966).
- ¹⁰L. Pueyo and J. W. Richardson, *J. Chem. Phys.* **67**, 3583 (1977).
- ¹¹H. Setyono and U. Scherz, *Phys. Rev. B* **33**, 3090 (1986).
- ¹²M. Blume and R. E. Watson, *Proc. R. Soc. London, Ser. A* **270**, 127 (1962).
- ¹³M. Blume and R. E. Watson, *Proc. R. Soc. London, Ser. A* **271**, 565 (1963).
- ¹⁴E. Francisco and L. Pueyo, *Phys. Rev. A* **36**, 1978 (1987).
- ¹⁵J. W. Richardson, T. F. Soules, D. M. Vaught, and R. R. Powell, *Phys. Rev. B* **4**, 1721 (1971).
- ¹⁶E. U. Condon and G. H. Shortley, *The Theory of Atomic Spectra* (Cambridge University Press, Cambridge, 1970).
- ¹⁷S. Sugano and R. G. Shulman, *Phys. Rev.* **130**, 517 (1963).
- ¹⁸J. W. Richardson, W. C. Nieuwpoort, R. R. Powell, and W. Edgell, *J. Chem. Phys.* **36**, 1057 (1962).
- ¹⁹H. Horie, *Prog. Theor. Phys.* **10**, 296 (1953).
- ²⁰B. W. N. Lo, K. M. S. Saxena, and S. Fraga, *Theor. Chim. Acta* **25**, 97 (1972).
- ²¹T. M. Dunn and Wai-Kee Li, *J. Chem. Phys.* **46**, 2907 (1967).
- ²²E. Clementi and C. Roetti, *At. Data Nucl. Data Tables* **14**, 177 (1974).
- ²³J. W. Richardson, R. R. Powell, and W. C. Nieuwpoort, *J. Chem. Phys.* **38**, 796 (1963).
- ²⁴L. Seijo, Z. Barandiarán, V. Luaña, and L. Pueyo, *J. Solid State Chem.* **61**, 269 (1986).
- ²⁵V. Luaña, G. Fernández Rodrigo, E. Francisco, L. Pueyo, and M. Bermejo, *J. Solid State Chem.* **66**, 263 (1987).
- ²⁶B. L. Kalman and J. W. Richardson, *J. Chem. Phys.* **55**, 4443 (1971).
- ²⁷V. Luaña, E. Francisco, M. Flórez, J. M. Recio, and L. Pueyo, *J. Chim. Phys. (Paris)* **84**, 863 (1987).
- ²⁸M. T. Barriuso and M. Moreno, *Phys. Rev. B* **29**, 3623 (1984).
- ²⁹V. Luaña, G. Fernández Rodrigo, M. Flórez, E. Francisco, J. M. Recio, J. F. Van der Maelen, L. Pueyo, and M. Bermejo, *Cryst. Lat. Def. Amorph. Mat.* (to be published).
- ³⁰M. Flórez, G. Fernández Rodrigo, E. Francisco, V. Luaña, J. M. Recio, J. F. Van der Maelen, L. Pueyo, M. Bermejo, M. Moreno, J. A. Aramburu, and M. T. Barriuso, *Cryst. Lat. Def. Amorph. Mat.* (to be published).
- ³¹A. Mehra and P. Venkateswarlu, *J. Chem. Phys.* **47**, 2334 (1967).
- ³²K. Y. Wong, N. B. Manson, and G. A. Osborne, *J. Phys. Chem. Solids* **38**, 1017 (1977).
- ³³J. Ferguson, H. J. Guggenheim, and D. L. Wood, *J. Chem. Phys.* **54**, 504 (1971).
- ³⁴E. Francisco, M. Flórez, G. Fernández Rodrigo, V. Luaña, J. M. Recio, M. Bermejo, and L. Pueyo, *Cryst. Lat. Def. Amorph. Mat.* **15**, 45 (1987).
- ³⁵L. Seijo and L. Pueyo, *J. Solid State Chem.* **56**, 241 (1985).
- ³⁶M. Flórez, L. Seijo, and L. Pueyo, *Phys. Rev. B* **34**, 1200 (1986).
- ³⁷G. Racah and Y. Shadmi, *Bull. Soc. Counc. Israel* **8F**, 15 (1959).
- ³⁸S. Fraga, J. Karwowski, and K. M. S. Saxena, *Handbook of Atomic Data* (Elsevier, Amsterdam, 1976).